JOURNAL OF BACTERIOLOGY, Feb. 1985, p. 478–483
0021-9193/85/020478-06$02.00/0

Vol. 161, No. 2

Confocal Scanning Light Microscopy of the *Escherichia coli* Nucleoid: Comparison with Phase-Contrast and Electron Microscope Images

J. A. C. VALKENBURG, C. L. WOLDRINGH, G. J. BRAKENHOFF, H. T. M. VAN DER VOORT, AND N. NANNINGA*

Department of Electronmicroscopy and Molecular Cytology, University of Amsterdam, Amsterdam, The Netherlands

Received 10 September 1984/Accepted 11 November 1984

The nucleoid of living and OsO_4- or glutaraldehyde-fixed cells of *Escherichia coli* strains was studied with a phase-contrast microscope, a confocal scanning light microscope, and an electron microscope. The trustworthiness of the images obtained with the confocal scanning light microscope was investigated by comparison with phase-contrast micrographs and reconstructions based on serially sectioned material of DNA-containing and DNA-less cells. This comparison showed (i) higher resolution of the confocal scanning light microscope as compared with the phase-contrast microscope, and (ii) agreement with results obtained with the electron microscope. The effects of fixation on the structure of the nucleoid were studied in *E. coli* B/r H266. Confocal scanning light micrographs and electron microscopic reconstructions showed that the shape of the nucleoid remained similar after OsO_4 or glutaraldehyde fixation; however, the OsO_4 nucleoid appeared to be somewhat smaller and more centralized within the cell.

The shape of the bacterial nucleoid remains to be determined because resolution of traditional light microscopy (LM) is low and because fixation and dehydration procedures necessary for electron microscopy (EM) change the appearance of the nucleoid (for a review, see C. L. Woldringh and N. Nanninga, *in* N. Nanninga, ed., *Molecular Cytology of Escherichia coli*, in press). In living bacteria studied with a phase-contrast LM, the nucleoid is visible as a cloudlike structure without much detail (10, 15). After fixation with OsO_4 under the conditions developed by Kellenberger et al. (8), a confined nucleoid can be observed in thin-sectioned cells, whereas after glutaraldehyde fixation, the nucleoid appears to be dispersed (9, 16, 17). Freeze-fracturing could not confirm the reliability of the results obtained with either fixative because of ice crystals present in the nucleoplasmic region and because the presence of freeze-protecting agents probably causes rearrangement of nucleoplasmic and cytoplasmic components (12, 19).

For study of the nucleoid in living cells and for examination of the effects of fixation on the morphology of the nucleoid at higher resolution, the confocal scanning light microscope (CSLM) was developed in our laboratory (2–4). The gain in resolution with the CSLM as compared with the traditional LM was demonstrated by Brakenhoff et al. (2, 3). In a recent biological application of CSLM, the banding pattern of a segment of *Drosophila hydei* was studied (6). An increase of 60% in the number of visible bands was demonstrated.

With the better resolution of the CSLM, additional details in the overall shape and substructure of the nucleoid could be expected and have, in fact, preliminarily been shown (3). The extra detail visible in CSLM images of bacteria, however, might be of a spurious nature. To investigate this problem further, we studied a temperature-sensitive gyrase B mutant of *Escherichia coli*. Shifting cells of this strain to 42°C leads to the formation of two types of cells: large, DNA-containing filaments and small, DNA-less cells (13).

Comparison of CSLM images with phase-contrast micrographs and reconstructions based on serially sectioned material was used to compare the effects of OsO_4 and glutaraldehyde fixation on the morphology of the nucleoid in wild-type *E. coli* cells. Our results indicate that although large differences can be observed between thin sections of OsO_4- or glutaraldehyde-fixed cells, the overall shape of the nucleoid is similar after fixation with either fixative. However, the glutaraldehyde nucleoid appears less confined to the cell center than the OsO_4-fixed one. The often described dispersed character of the glutaraldehyde nucleoid in thin sections appears misleading, possibly because of the presence of transcription-translation complexes (ribosomes) around its circumference (5) and because of a retention of proteins (16a).

MATERIALS AND METHODS

Bacterial strains, media, and growth conditions. The *E. coli* strains used were the wild-type strain B/r H266 (obtained from P. G. de Haan, University of Utrecht) and the thermosensitive gyrase B mutant LE316 (obtained from I. B. Holland, University of Leicester). Cells were grown in batch culture in a synthetic medium according to Helmstetter and Cooper (7), supplemented with 1% tryptone and 0.5% yeast extract. B/r H266 cells were grown at 37°C for at least eight generations (doubling time [T_D], 21 min). LE316 cells were grown at 30°C (permissive temperature; T_D, 36 min) for at least eight generations and then were shifted to 42°C (restrictive temperature).

Fixation and EM. Cells were prefixed by adding to the culture medium OsO_4 to a final concentration of 0.1% or glutaraldehyde to a final concentration of 2.5% (vol/vol). The OsO_4-prefixed cells were postfixed after 15 min; the glutaraldehyde-prefixed cells were postfixed after 60 min. Postfixation was performed by the Ryter-Kellenberger technique (8)

* Corresponding author.

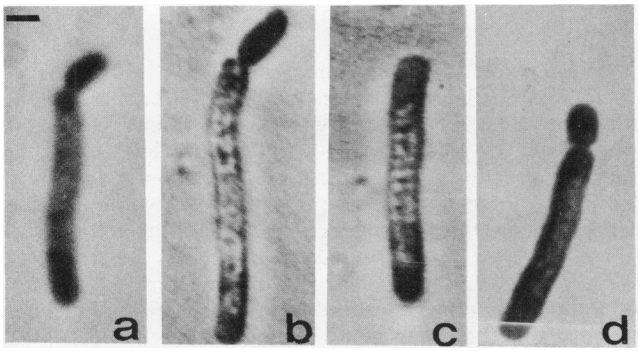

FIG. 1. *E. coli* LE316 shifted from 30 to 42°C and grown for 60 min at 42°C. Shown are phase-contrast LM (a) and CSLM (b to d) images of living (a to c) and OsO_4-fixed (d) cells. Bar, 1 μm.

by suspending the cells in 0.1% tryptone–1% OsO_4 in acetate-Veronal buffer (pH 6.0) containing 0.12 M NaCl, 0.01 M $MgCl_2$, and 0.1% tryptone, followed by further fixation in 1.0% uranyl acetate in the same buffer. For CSLM and phase-contrast microscopy, cells were resuspended in buffer. For EM, cells were dehydrated in ethanol and embedded in araldite. Sections of the embedded material were cut on an LKB ultramicrotome (LKB Instruments Inc., Rockville, Md.) with a glass knife. After being stained with uranyl acetate and lead citrate (14), the sections were examined in a Philips 300 EM. Three-dimensional models were constructed based on prints of serially sectioned cells.

LM. Living and fixed cells were prepared for the phase-contrast and confocal scanning light microscopes according to Binnerts et al. (1). In short, cells were allowed to adhere to object slides coated with 0.01% poly-L-lysine and immersed in solutions of bovine serum albumin (column fraction V; Sigma Chemical Co., St. Louis, Mo.) in growth medium. The refractive index of these solutions was measured with an Abbe type refractometer. For phase-contrast microscopy, a "Wild" (Wild, Heerbrugg, Switzerland) positive Zernike contrast microscope was used.

CSLM. The design of the CSLM has been published previously (2, 4). In this microscope, two objective lenses are placed with their focal planes coinciding (the confocal arrangement). A laser beam is focused into a point with one objective lens and directed to a photomultiplier with the aid of a second objective lens. Absorption is measured as a

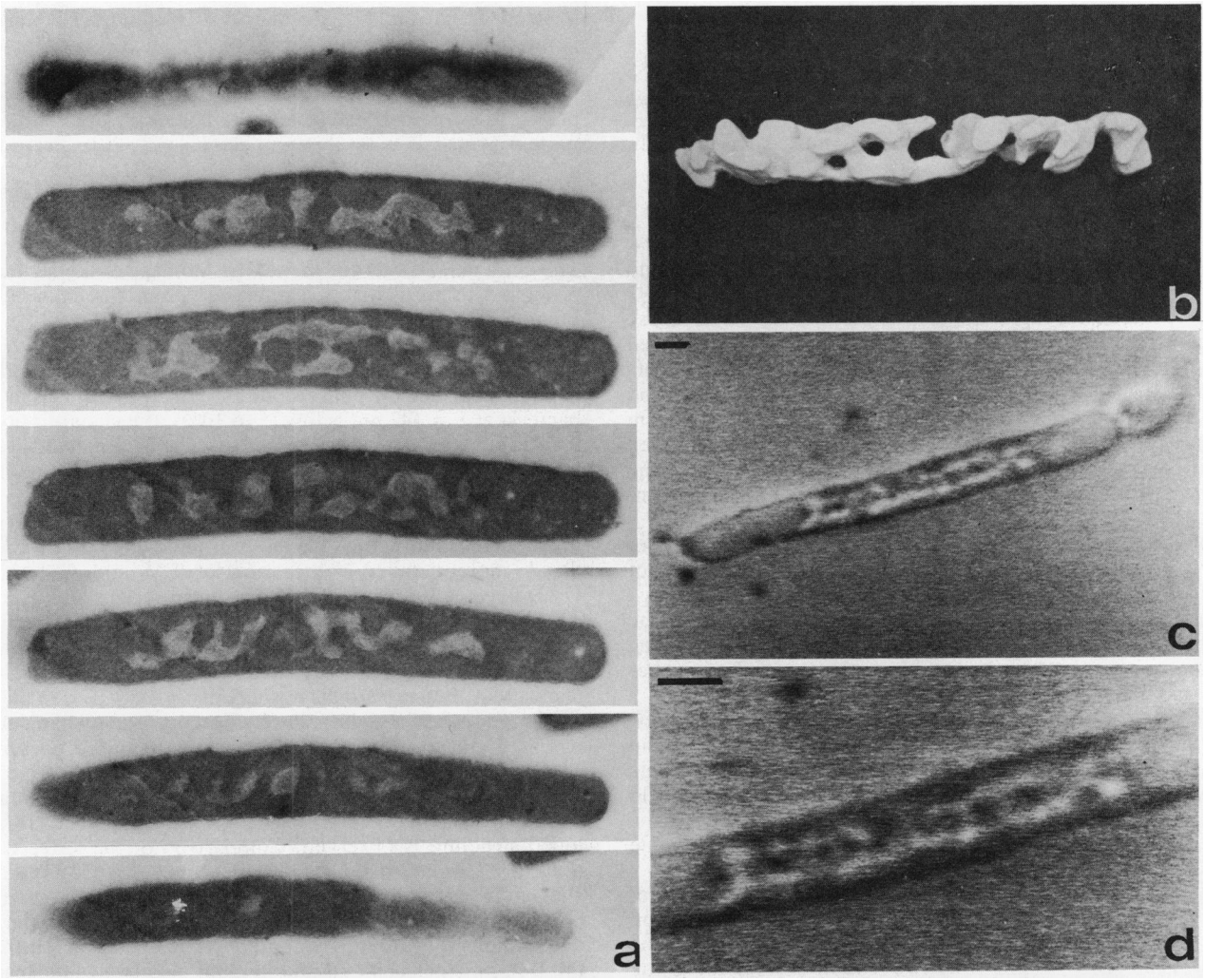

FIG. 2. *E. coli* LE316 shifted from 30 to 42°C and grown for 60 min at 42°C. This figure shows a comparison of CSLM images of living cells (c and d) with a reconstruction of an OsO_4-fixed nucleoid (b), based on serial sections (a) studied with the EM. Bar, 1 μm.

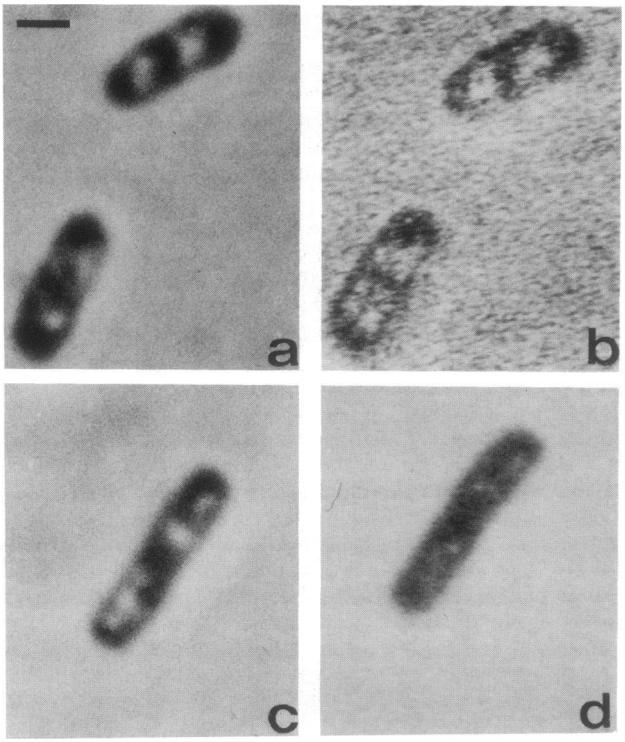

FIG. 3. Fast-growing *E. coli* B/r H266 (T_D, 21 min), showing a comparison of phase-contrast LM (a, c) with CSLM (b and d) images of the same living (a and b) and OsO_4-fixed (c and d) cells. Bar, 1 μm.

preparation is moved through the coinciding focal points. The photomultiplier signals are electronically processed and translated into a video image. A HeCd laser operating at 442 nm was used throughout these experiments. Under these circumstances, a point resolution of 150 nm can be obtained (3, 4). At this wavelength, absorption of living cells amounts to 5 to 10%. To prevent the formation of dark halos around the cells, it is necessary to immerse bacteria in a medium with a refractive index that approaches the refractive index of these bacteria (3). This makes it possible to study the same cell under the same conditions with both phase-contrast LM and CSLM.

Image processing. The electronic signal processing of the CSLM makes contrast enhancement and filtering of images possible. In this investigation, the following two types of filtering were used. During acquisition of the image, the object was scanned several times, the resulting image being the result of four to eight scans. For further improvement of the signal-to-noise ratio, a spatial 3 × 3 Gauss filter was applied to the image (the value of a new picture element is the weighed average of the element in an area consisting of the original element and the eight elements surrounding it). With the magnification used, this filter did not affect the resolution or information content of the images. After filtering, contrast was enhanced to a suitable level.

Electron micrographs of thin-sectioned, glutaraldehyde-fixed cells were 9 × 9 Gauss filtered. The resulting resolution in these images was comparable to the resolution in the CSLM images. In this way we could, by reducing the information content (i.e., the removal of ribosomes), compare electron micrographs with CSLM micrographs.

RESULTS

DNA-less and DNA-containing cells. DNA-less cells produced after the temperature-sensitive gyrase B mutant LE316 was cultivated at 42°C showed no extra internal structure when viewed by CSLM (Fig. 1). This is evidence that no spurious structures are created in a cell not containing DNA. However, it might be possible that in DNA-containing cells, artifactual structures arise because of an undefined interaction of the laser beam with the nucleoid or its surroundings. We have studied this problem also with the gyrase B mutant. Inhibition of gyrase B does not prevent cell elongation, and the nucleoid becomes centrally located in the cell (13). Figures 1b, c, and d show the increase in detail obtained by CSLM as compared with the phase-contrast LM image (Fig. 1a). This increase in resolution is visible in unfixed cells (Fig. 1b and c) as well as in OsO_4-fixed cells (Fig. 1d). The configuration is a typical arrangement composed of lobed structures, sometimes resembling a ladder. To assess this structure further, we made a three-dimensional model of the "gyrase nucleoid" from serial sections of OsO_4-fixed cells (Fig. 2a). This EM-based model (Fig. 2b) also has a lobed or a somewhat ladder-like structure and as such resembles quite well the CSLM image (Fig. 2c and d). In the terminology of Hobot et al. (J. A. Hobot, W. Villiger, J. Villiger, J. Escaig, M. Maeder, A. Ryter, and E. Kellenberger, manuscript in preparation), we might say that the gyrase nucleoid represents a physiological state which is not so much affected by preparation procedures. (Another example is the rounded nucleoid obtained after inhibition of protein synthesis with chloramphenicol [11, 20]). From the above comparison, we infer that the CSLM images of the gyrase nucleoid do not contain recognizable artifactual structures.

Osmium tetroxide-fixed cells and glutaraldehyde-fixed cells. The extra detail observed in the CSLM image of the nucleoid prompted us to use it as a reference point for fixed cells. Figures 3a and b show images of *E. coli* B/r H266 (T_D, 21 min) made by phase-contrast LM and CSLM, respectively. In the latter case, image formation is based on absorption contrast and not on phase contrast. As the absorption by bacteria at $\lambda = 442$ nm is low (5 to 10%), the signal-to-noise ratio is low as well. This appeared less the case in fixed cells, in which the absorption amounted to 20 to 25%, probably because of an addition of fixative to the cells (16a). In CSLM, the outline of the nucleoid is more defined in living cells (Fig. 3a and b) but also in OsO_4-fixed cells (Fig. 3c and d). A more detailed comparison of EM and CSLM of OsO_4-fixed cells is shown in Fig. 4. From serial sections (not shown) of the cell of Fig. 4a, a spatial model was made (Fig. 4b). This model is a lobed structure with a hole in the center. Comparison with the OsO_4-fixed CSLM nucleoid (Fig. 4c) shows that they are similarly shaped.

The analysis of the glutaraldehyde image is shown in detail in Fig. 5. Figure 5b shows a spatial model based on serial sections (not shown) of the cell in Fig. 5a. The shape of this model in principle resembles quite well the CSLM image of a glutaraldehyde-fixed cell (Fig. 5c). In both cases, a lobed structure is observed. Comparison of the latter with the LM phase-contrast image of the same cell (Fig. 5d) again shows the gain in resolution obtained by CSLM, the nucleoid being more distinct in the CSLM image. The glutaraldehyde image of the nucleoid appears less contracted than the OsO_4 images (Fig. 3d and 4c) and also comes closer to the nucleoid image of the living cell (Fig. 3b). In the fast-growing *E. coli* cells studied here, the nucleoid is not so

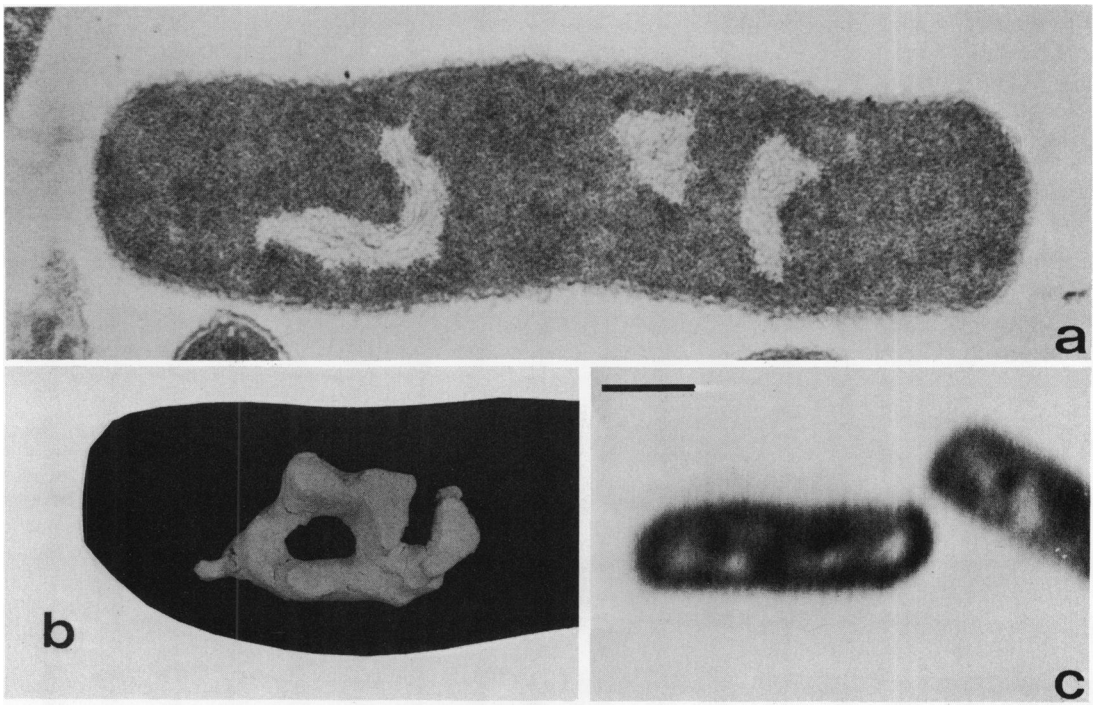

FIG. 4. Fast-growing *E. coli* B/r H266 (T_D, 21 min), showing a comparison of a CSLM micrograph of an OsO_4-fixed cell (c) with a reconstruction of an OsO_4-fixed nucleoid (b), based on serial sections studied with the EM. Only one of these sections is shown here (a). Bar, 1 μm.

centrally located but occurs often in the vicinity of the cell envelope.

Image processing of electron micrographs of glutaraldehyde-fixed cells. From the foregoing, the glutaraldehyde nucleoid appears as a distinct structure, clearly larger than the OsO_4 nucleoid; the dispersed appearance of the glutaraldehyde-fixed nucleoid presumably is caused by the presence of protein complexes (16a). To further verify this notion, we subjected electron micrographs of glutaraldehyde-fixed cells to image processing (Fig. 5e and f). This was done in such a way as to remove the ribosomes from the image. Of course, this leads to a loss of information, but it gives an impression of how cells would look in the absence of ribosomes. The obtained result (Fig. 5f) shows a somewhat complex though lobed structure that is quite reminiscent of the CSLM micrograph (Fig. 5c). This analysis shows that the nucleoid in these fast-growing, glutaraldehyde-fixed cells comes near the envelope (in contrast to the more central location of the OsO_4-fixed nucleoid; Fig. 4).

DISCUSSION

Our main goal in developing the CSLM was to study hydrated biological specimens in a living state at a higher resolution than has been obtained by conventional LM. With the CSLM, a point resolution of 150 nm can be obtained by using a HeCd laser operated at $\lambda = 442$ nm (3, 4).

In the case of the nucleoid, the higher resolution manifests itself in the sense that a cloudlike structure becomes a lobed structure (or, in the terminology of Hobot et al. [manuscript in preparation], "more cleft in appearance"). It should be realized that the nucleoid morphology here described applies to *E. coli* B/r H266 cells growing with a T_D of 21 min; i.e., multifork replication takes place and cells contain between two and four nucleoids. At slower growth, the nucleoid assumes a more simple structure (18). In the phase-contrast LM, an *E. coli* cell oriented with its long axis perpendicular to the optical axis lies completely within the focal plane. In the CSLM, operating at $\lambda = 442$ nm, the depth of the focal plane is ca. 0.4 μm; and almost the complete nucleoid is visualized. This means that CSLM micrographs are best compared with reconstructions of nucleoids based on electron micrographs of serial sections. The close agreement between the CSLM micrographs (Fig. 2c, 4c, and 5c) and the pictures of reconstructions (Fig. 2b, 4b, and 5b) demonstrate the reliability of image formation in CSLM. In addition, no spurious structures were seen in DNA-less cells (Fig. 1).

In recent years, sufficient evidence has accumulated for us to accept as a general conclusion that the OsO_4 nucleoid is more confined than in the in vivo situation (for a review and references, see Woldringh and Nanninga, in press). The main arguments are that OsO_4 fixation changes the ionic environment of the DNA (12) and disrupts the association of DNA with proteins (16a) and transcription-translation complexes (5). Therefore, we will mainly be concerned with the interpretation of glutaraldehyde nucleoid. The shape of that nucleoid is similar to the one obtained after OsO_4 fixation, but it is less contracted. As a consequence, the glutaraldehyde nucleoid comes close to the vicinity of the cell envelope. This is also clearly seen in CSLM images of living cells (Fig. 3b) as well as in glutaraldehyde-fixed cells (Fig. 5c). The dispersed appearance of glutaraldehyde nucleoid is most likely caused by the presence of transcription-translation complexes at the boundary of nucleoid and cytoplasm. If ribosomes are removed by image processing (Fig. 5g), a more confined nucleoid picture emerges which is quite reconcilable with the CSLM images of living cells. The glutaraldehyde nucleoid therefore comes most close to reality as far as size and shape are concerned. However, considerably more work has to be done regarding the definite interpretation of the election microscope image.

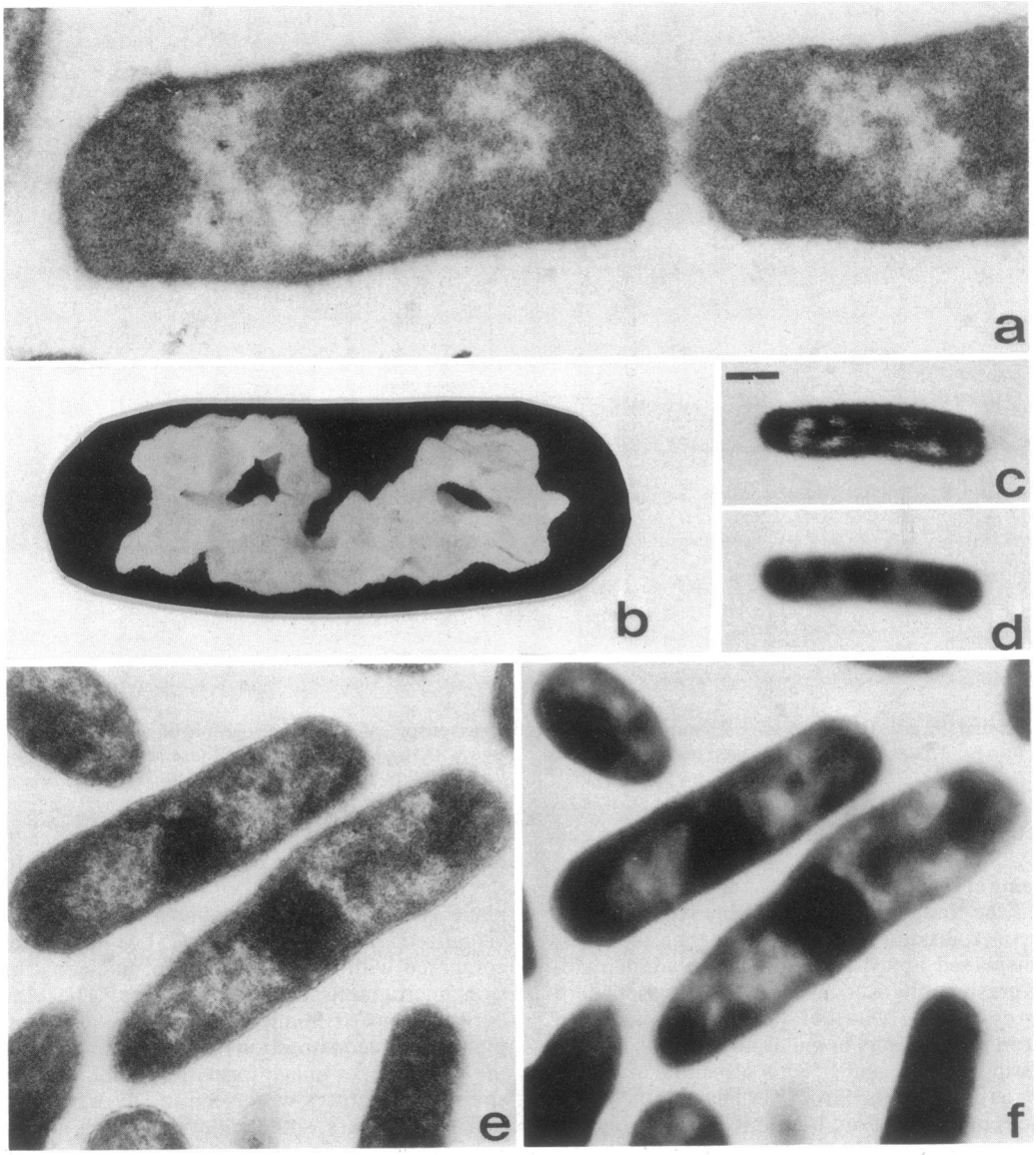

FIG. 5. Fast-growing *E. coli* B/r H266 (T_D, 21 min), showing a comparison of a CSLM micrograph of a glutaraldehyde-fixed cell (c) with a phase-contrast light micrograph of the same cell (d) and with a reconstruction of a glutaraldehyde-fixed nucleoid (b), based on serial sections studied with the EM. Only one of these sections is shown here (a). Panel f shows the electron micrograph of glutaraldehyde-fixed cells (e) after image processing (for further details, see the text). Bar, 1 μm.

ACKNOWLEDGMENTS

We thank J. Leutscher and E. van Spronsen for assistance in preparing the figures.

This investigation was supported in part by the Foundation for Fundamental Biological Research (BION), which is subsidized by the Netherlands Organisation for the Advancement of Pure Research (ZWO).

LITERATURE CITED

1. **Binnerts, J. S., C. L. Woldringh, and G. J. Brakenhoff.** 1982. Visualisation of the nucleoid in living bacteria on poly-lysine coated surfaces by the immersion technique. J. Microsc. **125**:359–363.
2. **Brakenhoff, G. J.** 1979. Imaging modes in confocal scanning light microscopy (CSLM). J. Microsc. **117**:233–242.
3. **Brakenhoff, G. J., J. S. Binnerts, and C. L. Woldringh.** 1980. Developments in high resolution confocal scanning light microscopy (CSLM), p. 123–200. *In* E. A. Ash (ed.), Scanned image microscopy. Academic Press, London.
4. **Brakenhoff, G. J., P. Blom, and P. J. Barends.** 1979. Confocal scanning light microscopy with high aperture lenses. J. Microsc. **117**:219–232.
5. **Daneo-Moore, L., D. Dicker, and M. L. Higgins.** 1980. Structure of the nucleoid in cells of *Streptococcus faecalis*. J. Bacteriol. **141**:928–937.
6. **Grond, C. J., J. Derksen, and G. J. Brakenhoff.** 1982. The banding pattern of the segment 46A-48C in *Drosophila hydei* polutene chromosomes as studied by confocal scanning light microscopy. Exp. Cell Res. **138**:458–462.
7. **Helmstetter, C. E., and S. Cooper.** 1968. DNA synthesis during the division cycle of rapidly growing *Escherichia coli* B/r. J. Mol. Biol. **31**:507–518.
8. **Kellenberger, E., A. Ryter, and J. Séchaud.** 1958. Electron microscope study of DNA-containing plasms. II. Vegetative and mature phage DNA as compared with normal bacterial nucleoids in different physiological states. J. Biophys. Biochem. Cytol. **4**:671–676.

9. **Margaretten, W., C. Morgan, H. S. Rosenkranz, and H. M. Rose.** 1966. Effect of hydroxyurea on virus development. I. Electron microscopic study of the effect on the development of bacteriophage T4. J. Bacteriol. **91**:823–833.
10. **Mason, D. J., and D. M. Powelson.** 1956. Nuclear division as observed in live bacteria by a new technique. J. Bacteriol. **71**:474–479.
11. **Morgan, C., H. S. Rosenkranz, H. S. Carr, and H. M. Rose.** 1967. Electron microscopy of chloramphenicol-treated *Escherichia coli*. J. Bacteriol. **93**:1987–2002.
12. **Nanninga, N., and C. L. Woldringh.** 1981. The interpretation of chemically fixed and freeze-fractured bacterial nucleoplasm. Acta Histochem. Suppl. **23**:39–53.
13. **Orr, E., N. F. Faitweather, I. B. Holland, and R. H. Pritchard.** 1979. Isolation and characterization of a strain carrying a conditional lethal mutation in the cou gene of *Escherichia coli* K12. Mol. Gen. Genet. **177**:103–112.
14. **Reynolds, E. S.** 1963. The use of lead citrate at high pH as an electron opaque stain in electron microscopy. J. Cell Biol. **17**:208–212.
15. **Schaechter, M., J. P. Williamson, J. R. Hood, and A. L. Koch.** 1962. Growth, cell and nuclear divisions in some bacteria. J. Gen. Microbiol. **29**:421–434.
16. **Séchaud, J., and E. Kellenberger.** 1972. Electron microscopy of DNA-containing plasms. IV. Glutaraldehyde-uranyl acetate fixation of virus-infected bacteria for thin sectioning. J. Ultrastruct. Res. **39**:598–604.
16a. **Valkenburg, J. A. C., and C. L. Woldringh.** 1984. Phase separation between nucleoid and cytoplasm in *Escherichia coli* as defined by immersive refractometry. J. Bacteriol. **160**: 1151–1157.
17. **Woldringh, C. L.** 1973. Effects of cations on the organisation of the nucleoplasm in *Escherichia coli* prefixed with osmium tetroxide or glutaraldehyde. Cytobiologie **8**:97–111.
18. **Woldringh, C. L.** 1976. Morphological analysis of nuclear separation and cell division during the life cycle of *Escherichia coli*. J. Bacteriol. **125**:248–257.
19. **Woldringh, C. L., and N. Nanninga.** 1976. Organization of the nucleoplasm in *Escherichia coli* visualised by phase-contrast light microscopy, freeze fracturing, and thin sectioning. J. Bacteriol. **127**:1455–1464.
20. **Zusman, D. R., A. Carbonell, and J. Y. Haga.** 1973. Nucleoid condensation and cell division in *Escherichia coli* MX74T2 *ts52* after inhibition of protein synthesis. J. Bacteriol. **115**:1167–1178.